

# IR, TPR, AND TPD STUDY OF SUPPORTED COBALT CATALYSTS —Effects of Metal Loading and Support Materials—

Jeong-Gil Choi, Hyun-Ku Rhee\*, and Sang Heup Moon<sup>†</sup>

Reaction Engineering Laboratory, Korea Advanced Institute of Science and Technology  
P.O. Box 131, Dongdaemun, Seoul, Korea

\* Department of Chemical Engineering, Seoul National University

(Received 14 May 1984, • accepted 9 July 1984)

**Abstract**—The surface properties of supported Co catalysts for different metal loading and support materials have been studied using Infrared Spectroscopy(IR), Temperature-Programmed Reduction(TPR), and Temperature-Programmed Desorption(TPD). Supported Co catalysts are more difficult to reduce than unsupported CoO powder, and the activation energy of reduction increases with reduced metal loading. This is because the highly dispersed, small metal particles interact strongly with the support material. The metal-support interaction varies with different support materials providing different activation energies of reduction and CO desorption properties. A strong compensation effect is observed for the catalyst reduction process.

## INTRODUCTION

Although many studies have been made on the catalytic properties of Group VIII metals in various reactions, there still remains much uncertainty in correlation between the surface properties of supported metal catalysts and their preparation methods. Previous studies have revealed wide variations in surface properties according to different preparation conditions [1]. In some cases, such variations have been regarded as to provide a clue to development of new catalysts [2].

An example is enhancement of catalytic activity and selectivity of TiO<sub>2</sub>-supported Ni catalysts in CO hydrogenation as compared to the catalysts using conventional support materials [2]. Vannice and Garten [3] reported that specific activity of methanation and product selectivity for C<sub>2</sub><sup>+</sup> hydrocarbons in CO hydrogenation were greatly enhanced on Ni/TiO<sub>2</sub> and metal particles [4].

Another example, although it is not directly correlated with activity results, is variation in IR spectra of CO molecules adsorbed on Co catalysts supported on different support materials. Queau and Poilblanc [5] have observed on Co film two IR bands at 1980 and 1880cm<sup>-1</sup>, the latter being intenser than the other. Blyholder and Allen [6] reported a similar result, but

their spectrum showed the opposite relative intensities of the two bands. The IR spectra on Co/SiO<sub>2</sub>, observed by Heal et al.[7], comprise two major bands: one at 2181cm<sup>-1</sup> and the other of doublet structure between 2032 and 2062cm<sup>-1</sup>. Kavtaradze and Sokolova [8] reported four IR bands on Co/Al<sub>2</sub>O<sub>3</sub>: 2140, 2070, 1950, and 1820cm<sup>-1</sup>.

A third example is variation in reducibility of supported metal catalysts with the amount of metal loading. Bartholomew et al. [9] have observed for Ni/SiO<sub>2</sub> that the extent of metal reduction increases from 29 to 97% as the metal loading is increased from 0.5 to 25%.

With the above background, we have made an extensive study on the effects of metal loading and support materials on the surface properties of Co catalysts using IR spectroscopy, Temperature-Programmed Reduction (TPR), and Temperature-Programmed Desorption (TPD).

## EXPERIMENTAL

### Materials

All cobalt catalysts were prepared using Co(NO<sub>3</sub>)<sub>2</sub>·6H<sub>2</sub>O obtained from the Ventron Corporation. The support materials used were: γ-Al<sub>2</sub>O<sub>3</sub>, SiO<sub>2</sub>, and SiO<sub>2</sub>-Al<sub>2</sub>O<sub>3</sub> obtained from the Ventron Corporation, and TiO<sub>2</sub> obtained from Cabot Corporation. The reported surface

<sup>†</sup> To whom all the correspondence should be made.

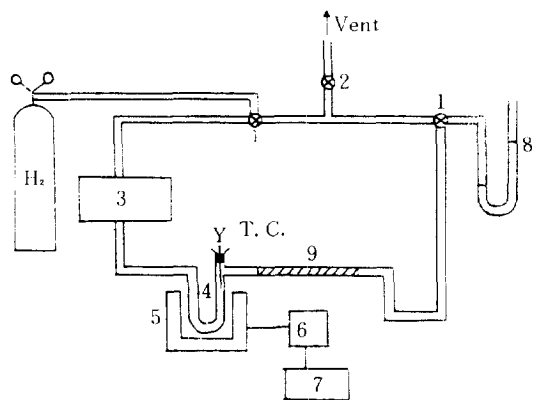
areas for each materials were 200, 600, 300, and 50m<sup>2</sup>/g, respectively. Hydrogen (Matheson ultra-high-purity 99.9995%) and helium (Matheson ultra-high-purity 99.999%) were further purified by flowing them through Deoxo unit (Engelhard Ind.) and Molecular Sieve 5A (Linde) traps. A Silica Gel Blue column was attached next to the molecular sieve trap as an indicator of regeneration period of the purification unit. Carbon monoxide (Takachiho Trading Co., Ltd., 99.95%) was flowed through a molecular sieve 5A trap to remove water and iron carbonyls.

### Catalyst Preparation

Five different catalysts were prepared: four of these consisted of a nominal 5 wt% of Co on  $\gamma$ -Al<sub>2</sub>O<sub>3</sub>, SiO<sub>2</sub>, SiO<sub>2</sub>-Al<sub>2</sub>O<sub>3</sub>, and TiO<sub>2</sub>, while the last was 12 wt% Co/ $\gamma$ -Al<sub>2</sub>O<sub>3</sub>. All the catalysts were prepared by aqueous incipient wetness technique [10] except for the Co/TiO<sub>2</sub> catalyst, which was prepared by excess water method due to negligible pore volume of TiO<sub>2</sub>. After impregnation with the solution of Co(NO<sub>3</sub>)<sub>2</sub> · 6H<sub>2</sub>O in distilled, deionized water, the catalysts were dried at 110-120°C for 12 hours, calcined in air at 500°C for 1 hour, and stored in a desiccator.

### Apparatus and Procedure

**IR Spectroscopy.** The IR cells used were same as those described by Moon et al.[11]. During the experiment, the catalyst wafer in the cell was reduced in situ in hydrogen stream, the cell was evacuated below 10<sup>-5</sup> Torr for an hour, CO gas was introduced in the cell, and the IR spectra of CO adsorbed on the catalyst were observed. Fourier Transform Infrared Spectrometer (FTIR) was used for the IR measurements.



- |                       |                         |
|-----------------------|-------------------------|
| 1. Three-way Stopcock | 6. Variable Transformer |
| 2. Two-way Stopcock   | 7. Thermo-controller    |
| 3. Circulation Pump   | 8. Manometer            |
| 4. Reactor            | 9. Water Trap           |
| 5. Furnace            |                         |

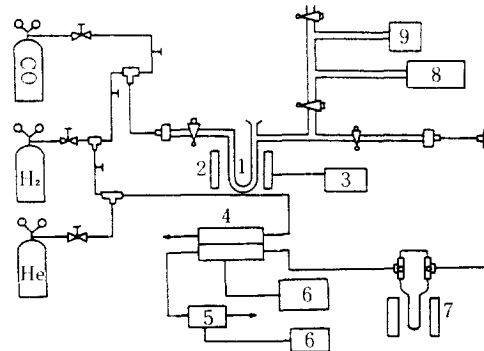
Fig. 1. Schematic Diagram of Temperature Programmed Reduction (TPR) Unit.

### Temperature-Programmed Reduction (TPR).

The TPR apparatus shown in Figure 1 is similar to one described by Robertson et al.[12]. The system is closed, and is made of glass except for the gas circulation part. The reactor is a simple U-shaped quartz tube with a thermocouple (iron-constantan) inserted thru a septum from the top. A water trap containing 0.5g of Silica Gel Blue and anhydrous magnesium perchlorate is connected next to the reactor to remove water produced by catalyst reduction. During the experiment, the system was filled with hydrogen, the reactor containing the catalyst sample was immersed into a tubular furnace for temperature control, and the internal gas, hydrogen, was circulated in the system using a Masterflex pump (Cole-Parmer model C-7520-00, Pump Head model C-7014-20). The internal volume of the TPR unit was 46cc, and the H<sub>2</sub> circulation rate was 25cc/min. Mass transfer resistance in the reaction system was considered insignificant because the space velocity was 2540hr<sup>-1</sup>. The extent of catalyst reduction was estimated by hydrogen pressure drop in the system as measured with a mercury manometer.

### Temperature-Programmed Desorption (TPD).

The TPD unit shown in Figure 2 is basically same as the TPR unit except that the desorption gas from the reactor is flowed through gas detectors for quantitative analysis. Since the desorption stream contained CO and CO<sub>2</sub>, two analyzers were used: gas chromatograph (Shimadzu model 3BT) without separation column for total analysis of CO and CO<sub>2</sub>, and CO analyzer (Horiba model Mexa-201) for CO only. The reactor was connected to an auxiliary vacuum unit to allow vacuum treatment of the catalyst. The general procedure of TPD experiment was as follows. Catalyst in the reactor was reduced in H<sub>2</sub> stream at elevated temperature, flushed with He for 30



- |                      |                               |
|----------------------|-------------------------------|
| 1. Reactor           | 6. Recorders                  |
| 2. Furnace           | 7. Liquid N <sub>2</sub> Trap |
| 3. Thermo-controller | 8. Meleod Gauge               |
| 4. Gas Chromatograph | 9. Mechanical Vacuum Pump     |
| 5. CO Analyzer       |                               |

Fig. 2. Schematic Diagram of Temperature Programmed Desorption (TPD) Unit.

minutes, and cooled to room temperature under vacuum. CO was then introduced into the reactor at 20cc/min for 30min, the reactor was evacuated again for 40 minutes, and He was flowed through the reactor at 110-125cc/min. The exit gas stream from the reactor was analyzed as the reactor temperature was increased linearly at 10°C/min.

## RESULTS

### Effect of Metal Loading

Figure 3 is a TPR result of the 5 wt% Co/Al<sub>2</sub>O<sub>3</sub> catalyst, which shows a typical trend of hydrogen pressure drop as the catalyst reduction proceeds at different temperatures. Data were taken at the initial period of reaction to eliminate possible complication due to a large pressure change. For each run at different temperatures, the initial hydrogen pressure was adjusted to 1 atm. The pressure drop directly represents the amount of catalyst reduction. An Arrhenius plot of the TPR result gives different activation energies of reduction for catalysts of different metal loading: 14.6 ± 2.0 kcal/gmol for 5 wt% Co/Al<sub>2</sub>O<sub>3</sub>, and 4.5 ± 0.5 kcal/gmol for 12 wt% Co/Al<sub>2</sub>O<sub>3</sub>.

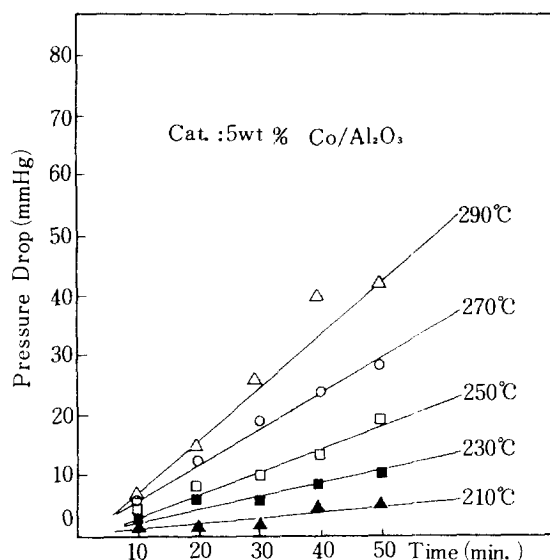


Fig. 3. Pressure Change with Time in TPR Experiment for 5 wt Co/Al<sub>2</sub>O<sub>3</sub>.

Figure 4 shows the TPD chromatogram of CO desorption from 5 wt% Co/Al<sub>2</sub>O<sub>3</sub> which was reduced in hydrogen at 550°C for 7 hours. The desorption band comprises many peaks, and they lose intensity as the TPD experiment is repeated on the same catalyst. Similar trend was observed on the 12 wt% catalyst, but in this case the initial intensity of the major band at

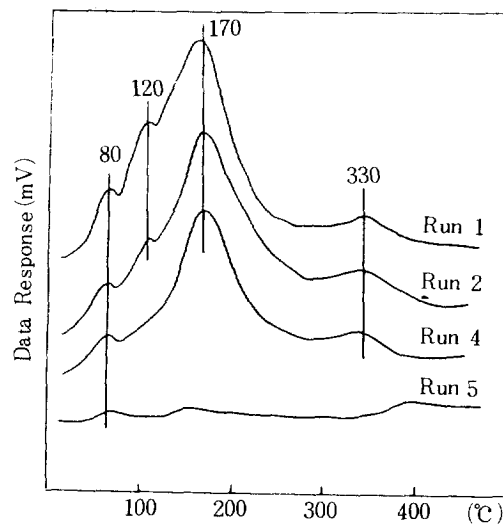


Fig. 4. TPD Chromatogram of CO Desorption from 5 wt Co/Al<sub>2</sub>O<sub>3</sub>.

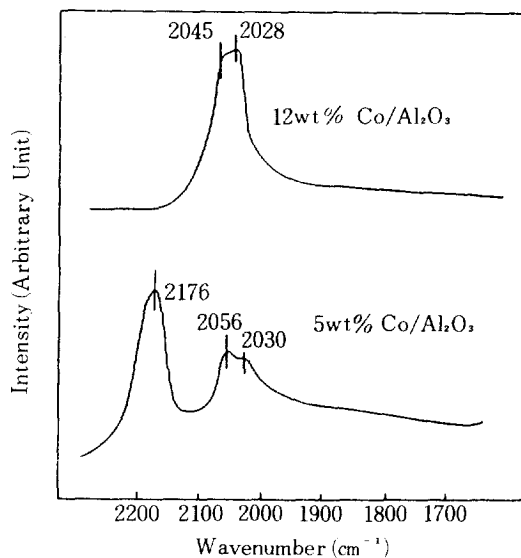


Fig. 5. IR Spectra of CO Adsorption on Co/Al<sub>2</sub>O<sub>3</sub>.

170°C was about 2/3 times smaller than that for the 5 wt% catalyst. Different amounts of the two sample catalysts were used in the TPD experiment so that weight of the metal component is same regardless of metal loading of the catalysts. Separate gas adsorption measurements showed that the 5 wt% catalyst adsorbed 2.6 times more CO than the 12 wt% catalyst for the same amount of metal component.

IR spectra of CO adsorbed on the two catalysts after they were reduced at 550°C for 17 hours are given in Figure 5. The 5 wt% catalyst shows two major bands:

one at  $2176\text{cm}^{-1}$  and the other band of doublet structure at  $2056$  and  $2030\text{cm}^{-1}$ . The 12 wt% catalyst shows only one band of doublet structure between  $2045$  and  $2028\text{cm}^{-1}$ .

### Effect of Support Materials

Activation energies of reduction, as measured by TPR, for four Co catalysts of different support materials,  $\text{SiO}_2$ ,  $\gamma\text{-Al}_2\text{O}_3$ ,  $\text{SiO}_2\text{-Al}_2\text{O}_3$ , and  $\text{TiO}_2$ , varied greatly as shown in Table 1. Sequence of catalysts in increasing activation energies is  $\text{Co/TiO}_2 < \text{Co/Al}_2\text{O}_3 < \text{Co/SiO}_2\text{-Al}_2\text{O}_3 < \text{Co/SiO}_2$ . Metal loading of each catalyst was 5 wt%, and temperature range of TPR experiments was between  $180$  and  $300^\circ\text{C}$ .

**Table 1.** Activation Energy of Reduction for various Co Catalysts.

Catalysts	Activation Energy (kcal/gmol)
$\text{Co/TiO}_2$	$6.7 \pm 1.2$
$\text{Co/Al}_2\text{O}_3$	$14.6 \pm 2.0$
$\text{Co/SiO}_2\text{-Al}_2\text{O}_3$	$15.0 \pm 0.8$
$\text{Co/SiO}_2$	$19.5 \pm 1.3$

TPD results of CO desorption, obtained after the catalysts were reduced at  $550^\circ\text{C}$  for 7 hours, are shown in Figure 6.  $\text{Co/Al}_2\text{O}_3$  shows an intense TPD chromatogram of complex structure with the band locations at  $80$ ,  $120$ ,  $170$ , and  $350^\circ\text{C}$ . For convenience, each band is designated as  $\alpha$ ,  $\beta$ ,  $\gamma$  and  $\delta$ , respectively.  $\text{Co/SiO}_2$  shows only  $\alpha$ -band, whereas only  $\beta$ -band is observed for  $\text{Co/SiO}_2\text{-Al}_2\text{O}_3$  and  $\text{Co/TiO}_2$ .

## DISCUSSION

### Effect of Metal Loading

TPR result showing a lower activation energy of reduction for 12 wt%  $\text{Co/Al}_2\text{O}_3$  than for the 5 wt% catalyst indicates that the catalyst becomes easily reduced as the metal loading increases. The trend coincides with the result of a separate experiment to reduce unsupported  $\text{CoO}$  powder, whose activation energy is  $4.1 \pm 2.0$  kcal/mol. This trend is same as the result of Bartholomew et al.[9] for  $\text{Ni/Al}_2\text{O}_3$ , who also observed that the extent of metal reduction at  $450^\circ\text{C}$  increased with the amount of metal loading. Recently, his group has reported [13] the same trend for their  $\text{Co/SiO}_2$  catalysts.

Easy reduction of Co catalysts with higher metal loading is also apparent from the IR result shown in Figure 5. It is commonly accepted that the bands occurring between  $2200$  and  $2140\text{cm}^{-1}$  are assigned to CO molecules physically adsorbed on metal oxides, whereas the bands between  $2100$  and  $2000\text{cm}^{-1}$  are due to CO molecules chemically bound to surface

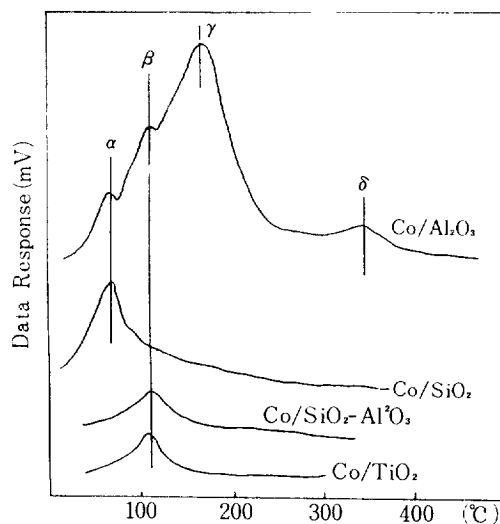


**Fig. 6.** TPD Chromatogram of CO for Various Co Catalysts.

metal [14]. Appearance of a band at  $2176\text{cm}^{-1}$  on 5 wt%  $\text{Co/Al}_2\text{O}_3$  indicates that the catalyst is partially reduced with some amount of Co oxides remaining on the catalyst surface. The  $2176$  band disappeared by evacuation, which supported that the band originated from physically adsorbed CO. Change of the bands below  $2100\text{cm}^{-1}$  by evacuation was minimal.

Larger amount of CO adsorption and desorption for the 5 wt% catalyst than for the 12 wt% catalyst as observed by separate gas adsorption measurements indicates that higher dispersion, hence smaller metal particles, was obtained on the lower loading catalyst. This was also confirmed by direct observation of the dispersed metal particles with transmission electron microscope (TEM). Similar trend of particle size increase with metal loading was also observed by Bartholomew et al.[9] for their  $\text{Ni/Al}_2\text{O}_3$  catalysts.

Conclusions from the above results are that Co particles dispersed on alumina are small for the catalyst of low metal loading, and that their reducibility by hydrogen becomes difficult as the dispersed Co particles become smaller. Since the catalysts were prepared by incipient wetness method, low metal loading means impregnation with solution of low cobalt concentration. Poor reduction of the Co catalyst may be due to strong interaction between the dispersed cobalt oxide particles and alumina support. Previous studies by Richardson [15] have revealed the  $\text{Co}^{+2}$  upon impregnation on  $\gamma\text{-Al}_2\text{O}_3$  becomes incorporated to some extent within the bulk of  $\gamma\text{-Al}_2\text{O}_3$ , forming a structure similar to that the spinel  $\text{Co(Al}_2\text{O}_4)$ . Such an interaction stabilizes the surface Co oxides, and this retards reduction of the catalyst.

The interaction will be stronger for highly dispersed small Co particles because they have more intimate contact with the support.

### Effect of Support Materials

Support materials in this study were selected to examine the effect of the following property of each material.

- 1)  $\text{Al}_2\text{O}_3$  forms, as previously mentioned, a stable compound with cobalt oxides [15].
- 2)  $\text{SiO}_2$  is generally regarded to be a relatively inert material providing minimal effect on the catalytic properties of the supported metal particles [16].
- 3)  $\text{TiO}_2$  is recently reported to make a strong interaction with transition metal (SMSI) [4].
- 4)  $\text{SiO}_2\text{-Al}_2\text{O}_3$  is the most acidic material among the four supports [17].

Activation energies of reduction measured in this study for different catalysts range from 6.7 to 19.5 kcal/gmol depending upon the support materials. These are higher than the value for unsupported Co oxide powder, 4.1 kcal/gmol, which suggests that reduction of cobalt oxide becomes more temperature-sensitive as the particle size becomes smaller by dispersion on the support. The reason for the high value of activation energy for  $\text{Co/SiO}_2$  is not clear presently, but this may be understood by extension of the results summarized by Eischens [18] for  $\text{Ni/SiO}_2$  catalyst. Here, they observed a strong interaction between dispersed nickel oxide and the silica support after reduction at temperatures above 500°C. They explained that this is due to formation of a stable nickel hydrosilicate during the reduction procedure. Same interaction may be expected for our  $\text{Co/SiO}_2$  catalyst.

If Polanyi relation [19], which designates linear relation between activation energy of reduction and logarithm of its heat of reaction, should hold for this series of catalysts, the equilibrium extent of reduction obtained by  $\text{H}_2$  reduction at elevated temperature should increase together with lowering of the reduction activation energy as follows:  $\text{Co/SiO}_2 < \text{Co/SiO}_2\text{-Al}_2\text{O}_3 < \text{Co/Al}_2\text{O}_3 < \text{Co/TiO}_2$ . However, according to the recent result of Zowtiak and Bartholomew [20] for their 3 wt% Co catalysts supported on different supports, the extent of reduction after treatment in  $\text{H}_2$  at 400°C for 16 hours increased in the order of  $\text{Co/TiO}_2 < \text{Co/Al}_2\text{O}_3 < \text{Co/SiO}_2$ . The order for 10 wt% catalysts was  $\text{Co/Al}_2\text{O}_3 < \text{Co/TiO}_2 < \text{Co/SiO}_2$ . This indicates that Polanyi relation does not hold in this case and therefore the activation energy of reduction is not directly related with the extent of reduction attainable by  $\text{H}_2$  reduction at elevated temperature.

Another observation in this study was that the catalyst reduction process exhibited a strong compensation effect as shown in Figure 7. The pre-exponential factor in Figure 7 was obtained by extrapolating the

reduction rate data to zero point of inverse temperature ( $1/T$ ). According to Figure 7, the reduction rate decreases significantly even if its activation energy is lowered by selection of a proper support material. The high extent of reduction of the high-activation-energy catalyst,  $\text{Co/SiO}_2$ , as reported by Zowtiak and Bartholomew [20], may be explained by this strong compensation effect.

The characteristic interaction of Co with different support materials may be understood from the TPD result shown in Figure 6. A separate study on the band occurring above 300°C for the  $\text{Co}/\gamma\text{-Al}_2\text{O}_3$  catalyst proved that the band was due to recombination of surface carbon with oxygen from the catalyst during the TPD experiment. This will be discussed in more detail in other paper [24]. The multi-band chromatogram below 300°C for  $\text{Co}/\gamma\text{-Al}_2\text{O}_3$  seems to represent a complex surface structure of the catalyst due to spinel formation in the reduction step.

Previous studies [21, 22, 23] have reported that upon impregnation Co first becomes attached to  $\gamma\text{-Al}_2\text{O}_3$  surface forming oxide compounds such as  $\text{Co}_3\text{O}_4$ . Calcination, especially at temperatures as high as 550°C, leads to diffusion of  $\text{Co}^{+2}$  ions into the interior of  $\gamma\text{-Al}_2\text{O}_3$ , the ions being positioned primarily at tetra-hedral or octahedral sites of  $\text{Al}_2\text{O}_3$ . Origin of the individual band in the chromatogram is not clear presently, but it is considered that different extent of catalyst reduction is related to the different CO desorption band.

Surface Co metal atoms combining with many neighboring oxygen atoms will desorb CO molecules at relatively low temperatures, whereas those combining with less oxygen atoms will desorb CO at high temperatures.

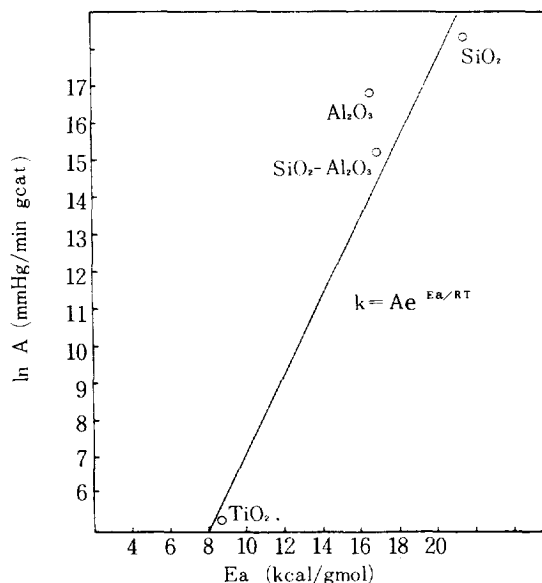


Fig. 7. Compensation Effect of Supported Co Catalysts.

Compounding of  $\text{Co}^{+2}$  ions with  $\text{Al}_2\text{O}_3$  in complex crystal structures may yield surface Co metal atoms combined with different number of oxygen atoms and consequently provide the observed complex TPD chromatogram.

Contrary to the case of  $\text{Co}/\text{Al}_2\text{O}_3$  catalyst, the other catalysts supported on  $\text{SiO}_2$ ,  $\text{SiO}_2\text{-Al}_2\text{O}_3$ , and  $\text{TiO}_2$  show a single band structure in their TPD chromatogram. The reason for that  $\text{Co}/\text{SiO}_2$  shows a band at the lowest temperature,  $\alpha$ -position, is not clear at the moment, but it is possible that the catalyst is the least reduced due to high activation energy of reduction. Occurrence of  $\beta$ -band for the other two catalysts may also be understood that they are moderately reduced with the reduced Co metal surrounded by many cobalt oxide molecules. Further study is required to explain different TPD chromatograms observed for the catalysts of different support materials.

### SUMMARY

Effects of metal loading and support materials on the surface properties of supported Co catalysts have been studied using experimental techniques such as IR, TPR, and TPD. The results showed that catalysts were more easily reduced when the metal loading was high. High dispersion of the surface metal component with lower metal loading was obtained. Different support materials made characteristic interactions with dispersed Co particles. Changes in activation energy of reduction and CO desorption properties were observed for catalysts of different support materials.

### Acknowledgement

This study was supported by Ministry of Science and Technology under the project No. of 6N00012.

### REFERENCES

1. Delmon, B., Grange, P., Jacobs, P., and Poncelet, G.: "Preparation of Catalysts II," Elsevier, New York (1979).
2. Vannice, M.A. and Garten, R.L.: U.S. Patent 4,042, 615, Aug. 16 (1977).
3. Vannice, M.A. and Garten, R.L.: *J. of Catal.*, **56**, 236 (1979).
4. Tauster, S.J., Fung, S.C. and Garten, R.L.: *J. Amer. Chem. Soc.*, **100**, 170 (1978).
5. Queau, R. and Poilblanc, R.: *J. Catal.*, **27**, 200 (1972)
6. Blyholder, G.E. and Allen, M.C.: *J. Amer. Chem. Soc.*, **91**, 3158 (1969).
7. Heal, M.J., Leisegang, E.C. and Torrington, R.G.: *J. Catal.*, **50**, 314 (1978).
8. Kavtaradze, N.N., and Sokolova, N.: *Russ. J. Phys. Chem.*, **38**, 548 (1964).
9. Bartholomew, C.H., Panell, R.B., Butler, J.L., and Mustard, D.G.: *Ind. Eng. Chem. Prod. Res. Dev.*, **20**, 296 (1981).
10. Palmer, M.B., Jr.: "The Effect of Preparation Variables on the Dispersion of Supported Pt Catalysts," Penn. State Univ., M. S. Thesis (1979).
11. Moon, S.H., Windawi, H. and Katzer, J.R.: *Ind. Eng. Chem. Fund.*, **20**, 396 (1980).
12. Robertson, S.D., McNicol, B.D., DeBaas, J.H. and Kloet, S.C.: *J. Catal.*, **37**, 424 (1975).
13. Reuel, R.C. and Bartholomew, C.H.: *J. Catal.*, **85**, 63 (1984).
14. Little, L.H.: "Infrared Spectra of Adsorbed Species", Chapt. 3, Academic Press, N.Y. (1966).
15. Richardson, J.T.: *Ind. Eng. Chem. Fund.*, **3**, 154 (1964).
16. Vannice, M.A.: *J. Catal.*, **50**, 228 (1977).
17. Tanabe, K.: "Solid Acids and Bases", Academic Press, N.Y. (1970).
18. Eischer, R.P., in E. Drauglis and Jaffee, R.I.: "The Physical Basis for Heterogeneous Catalysis," Plenum, N.Y. (1975) p. 485; Also, Satterfield, C.N., "Heterogeneous Catalysis in Practice," McGraw-Hill, N.Y., p. 80 (1980).
19. Boudart, M.: "Kinetics of Chemical processes," Prentice-Hall, Inc., NJ (1968).
20. Zowtiak, J.M. and Bartholomew, C.H.: *J. Catal.*, **83**, 107 (1983).
21. Ashley, J.H. and Mitchell, P.C.H.: *J. Chem. Soc.*, **15**, 2821 (1968).
22. Lipsch, J.M.M.G. and Schuit, G.C.A.: *J. Catal.*, **15**, 163 (1969).
23. Kiviat, F.E. and Petrakis, L.: *J. Phys. Chem.*, **77**, 1232 (1973).
24. Choi, J.G., Rhee, H-K. and Moon, S.H., in press